IAEA nuclear fusion

Importance of helical pitch parameter in LHD-type heliotron reactor designs

To cite this article: T. Goto *et al* 2011 *Nucl. Fusion* **51** 083045

Nucl. Fusion **51** (2011) 083045 (6pp) doi:10.1088/0029-5515/51/8/083045

Importance of helical pitch parameter in LHD-type heliotron reactor designs

T. Goto, Y. Suzuki, N. Yanagi, K.Y. Watanabe, S. Imagawa and A. Sagara

National Institute for Fusion Science, 322-6 Oroshi-cho, Toki, Gifu 509-5292, Japan

E-mail: goto.takuya@LHD.nifs.ac.jp

Received 31 December 2010, accepted for publication 6 July 2011
Published 29 July 2011
Online at stacks.iop.org/NF/51/083045

Abstract

One of the key issues in the design of LHD-type heliotron reactors is to secure sufficient blanket spaces. In this respect, helical pitch parameter γ is quite important because it significantly affects both the coil and plasma shapes. For a quantitative understanding of the effect of helical pitch parameter on a design window, a system design code for LHD-type heliotron reactors HELIOSCOPE (HELIOtron System design COde for reactor Performance Evaluation) is developed and parametric scans are carried out with three cases of $\gamma = 1.15$, 1.20 and 1.25. It became clear that design windows of heliotron reactors depend significantly on the engineering constraints: the stored magnetic energy of the coil system, the inboard minimum blanket space and the averaged neutron wall load. In the case of a fusion power of 3 GW, $\gamma = 1.20$ is optimum for relaxing physics requirements. But $\gamma = 1.15$ is also a possible selection if a lower fusion power or a higher neutron wall load is accepted. Since design windows are quite sensitive to the engineering constraints and physics conditions, a further detailed study on design feasibility of advanced engineering components and the effect of γ on the physics conditions is expected to optimize the value of γ.

1. Introduction

Helical systems with a net-current free plasma essentially have suitable properties as a DEMO and a commercial fusion reactor. There are no disruptive events in net-current free plasmas, resulting in the easiness in a steady-state operation. There is no need for a current drive power, leading to an increase in plant energy efficiency. In particular, the Large Helical Device (LHD) [1], a heliotron-type system with two continuous helical coils, has recorded several remarkable achievements, including high-beta (volume-averaged beta value $\langle\beta\rangle = 5.1\%$) discharges and extremely high central electron density ($n_{e0} > 10^{21}\,\mathrm{m}^{-3}$). Based on these achievements, a conceptual design of an LHD-type heliotron fusion reactor, FFHR (Force Free Helical Reactor) [2], has been advanced. One of the critical issues in the design of LHD-type heliotron reactors is to secure sufficient blanket space. Figure 1 shows the cross-sectional view of the coils and the magnetic surfaces including the ergodized layers of the magnetic field lines in vacuum on the poloidal cross-section at which the nested surfaces show a vertically elongated shape. Since these ergodized layers play an important role in the particle confinement, they should be considered as a plasma confinement region. The space between the helical coils and the plasma confinement region, i.e. the space for blanket, has its minimum at the inboard side on this cross-section. To expand the inboard minimum blanket space without changing the reactor size, a control of the cross-sectional shape of the magnetic surfaces is necessary. In an LHD-type heliotron system, there are two methods to control the shape of the magnetic surfaces. One is a control of multipole components of vertical magnetic field by adjusting the current in vertical field coils (VFCs). In particular, the dipole component determines the position of the magnetic axis R_{ax}. Outward shift of the magnetic axis expands the space between the helical coil and the last closed flux surface (LCFS) at the inboard side. However, the point in the ergodized layers closest to the inboard helical coil does not move so much with an outward shift of R_{ax}. Since the volume enclosed by the LCFS shrinks with an outward shift of R_{ax}, it leads to a degradation of the plasma confinement performance. On the other hand, it was found that the ergodized layers play an important role in the confinement of alpha particles [2], and the interference between the blanket and the ergodized layers should be avoided. Therefore, the outward shift of R_{ax} is not an effective method. In contrast, the helical pitch parameter γ has a relatively large effect on the expansion of the inboard minimum blanket space. The helical pitch parameter is defined as $\gamma = ma_c/\ell R_c$, where m, ℓ, a_c and R_c are the toroidal pitch number, poloidal pitch number, minor and major radii of helical coil(s), respectively. For an LHD-type ($\ell = 2$, $m = 10$) heliotron system, γ corresponds to the inverse aspect ratio of the helical coils (a_c/R_c). Therefore, a_c decreases with decreasing γ when R_c is kept constant. But the cross-sectional

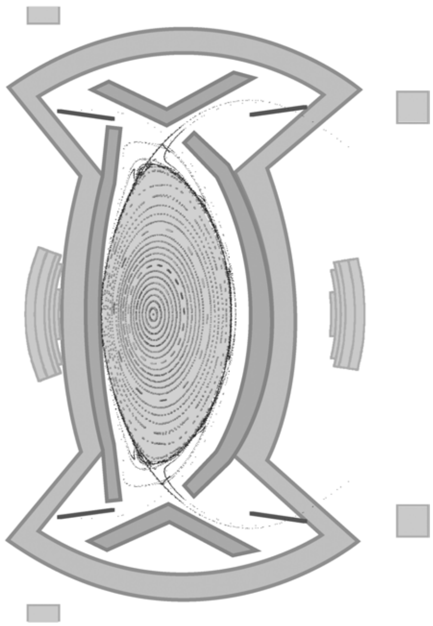

Figure 1. Cross-sectional view of magnetic surfaces, blankets, shields and coils of an LHD-type heliotron reactor at the vertically elongated cross-section with minimum blanket space at the inboard side.

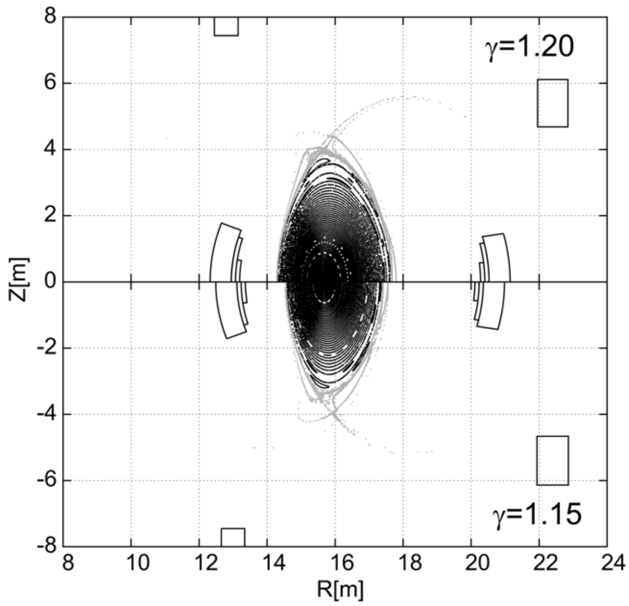

Figure 2. Comparison of the shapes of the external coils and the magnetic surfaces with helical pitch parameter γ of 1.20 (upper) and 1.15 (lower).

area of the magnetic surfaces including ergodized layers decreases more, and then the minimum inboard blanket space increases with decreasing γ (see figure 2). The reduction in γ also leads to a decrease in the magnetic hoop force on the helical coils. Therefore, the reduction in γ moderates the engineering design requirements. However, the decrease in the volume of the plasma confinement region leads to a degradation of the plasma confinement performance. In this respect, the effect of γ on the designs of LHD-type heliotron reactors needs to be investigated with a comprehensive standpoint on the overall reactor system. For a quantitative consideration of the relation between the design parameters, a system design code for LHD-type heliotron reactors, HELIOSCOPE (HELIOtron System design COde for reactor Performance Evaluation), is developed and parametric scans are carried out. In the next section, a brief review of HELIOSCOPE is given. Section 3 provides the result of the parametric scans.

2. Development of a system design code for heliotron reactors HELIOSCOPE

In the development of the system design code for heliotron reactors HELIOSCOPE, the most important and difficult issue is the evaluation of the shape of the magnetic surfaces. In contrast to tokamak reactors, the shape of the magnetic surfaces of heliotron reactors, especially the position of separatrices, is strongly coupled to the geometry of the external (helical) coils. Therefore, parameters related to the geometric configuration of the magnetic surfaces, which are needed to evaluate the plasma performance, cannot be given as input parameters but need to be obtained from an equilibrium calculation. Such an equilibrium calculation, however, is time consuming and cannot meet the computational speed fast enough for an application on parametric scans over a wide design space (less than 1 s for one parameter set). For this reason, a database of the magnetic surface configurations for various shapes of the helical coils with a fixed R_c is established separately using a field line tracing code and the 3D equilibrium code VMEC [3]. HELIOSCOPE refers this database and applies it to different values of R_c by a similar extension. In the design studies of FFHR, the number of pairs of VFCs reduced from 3 (for LHD) to 2 in order to secure large spaces for maintenance. In this study we also adopted two pairs of VFCs. It was found that, however, not only the geometry of the helical coils but also that of the VFCs significantly affects the geometry of magnetic surfaces including the ergodized layers. For this reason, the positions of the VFCs were carefully examined for each shape of the helical coils. Generally, VFCs of heliotron reactors are located on the circle whose centre is on the winding centre of the helical coils because of the easiness in the placement of supporting structures. At first the radius of the circle and the positions of the VFCs on the circle were determined to minimize the stored magnetic energy and the leakage field outside the torus. However, a field line tracing calculation clarified that the volume of the nested magnetic surfaces was ~15% smaller than that of the scale-up of LHD. Thereafter, the positions of the VFCs were adjusted to achieve as large a volume of the nested surfaces as possible without a significant increase in the stored magnetic energy. Figure 3 shows the comparison of the magnetic surface structures in the case of $\gamma = 1.2$ with the original and the modified positions of the VFCs.

In a heliotron system, an outward shift of the magnetic axis position with an increase in plasma pressure (Shafranov shift) has been theoretically predicted. Such an outward shift has also been observed in LHD high-beta discharges. The numerical simulations using the HINT2 code [4], which can calculate 3D equilibrium without an assumption of the existence of nested magnetic surfaces, have predicted that the volume of the nested surface shrinks with increasing plasma pressure due

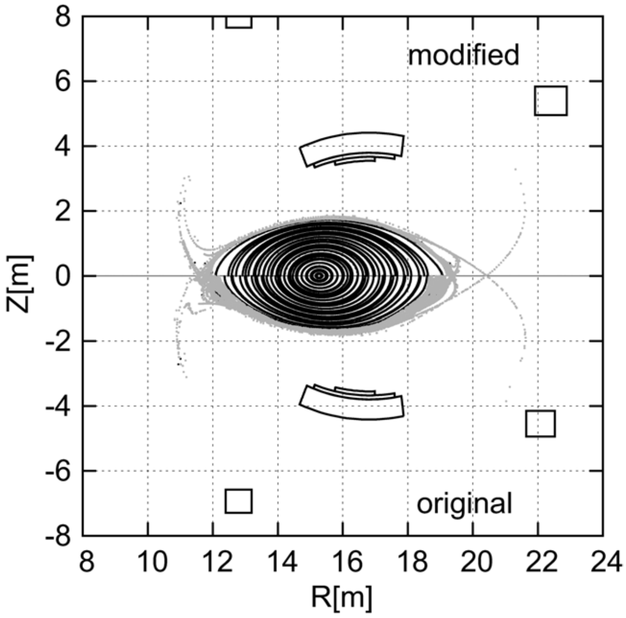

Figure 3. Comparison of the magnetic surface structures and the shape of the helical and vertical field coils with the original (lower) and the optimized (upper) positions of the VFCs.

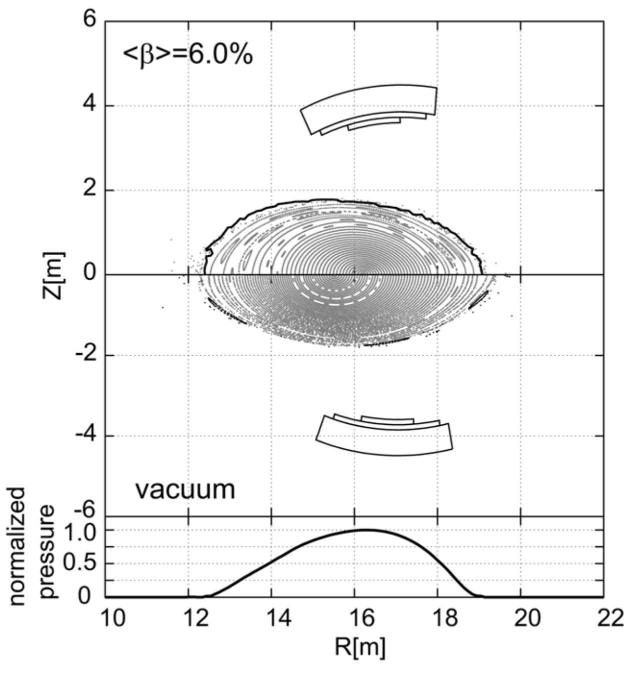

Figure 4. Comparison of the magnetic surface structure in vacuum (lower) and in a high-beta state (6.0% in volume-averaged value) with the adjustment of the vertical field. The solid line in the upper figure shows the pressure boundary. The bottom graph shows the normalized pressure profile.

to ergodization of the peripheral region [5]. However, such a decrease in the nested volume can be restored by applying an appropriate vertical field by controlling the current in the VFCs. Figure 4 shows the comparison of the magnetic surface structure in vacuum and in a high-beta state (6.0% in volume-averaged value) with the adjustment of the vertical field. In the high-beta case, a vertical field that makes the inward shift of the magnetic axis with a ratio between R_{ax} and R_c of 3.51/3.9 under the vacuum condition was applied. (On the other hand, $R_{ax}/R_c = 3.6/3.9$ in vacuum equilibrium.) The high-beta equilibrium was calculated using the HINT2 code. In this calculation, the pressure boundary was set on the magnetic field line with a connecting length of 1 km, which is sufficiently longer than the electron mean free path. The calculation result indicates that the Shafranov shift and the accompanying decrease in the nested surface volume can be effectively restored. The outermost surface becomes ergodized but the volume including finite pressure is almost the same as that of the LCFS in vacuum. This fact means a plasma volume as large as that of the LCFS in vacuum can be realized in a high-beta state. Therefore, all equilibrium calculations to establish the database of the magnetic field configurations were carried out with a vacuum equilibrium to reduce the computational time.

HELIOSCOPE consists of three main modules: engineering design module, physics design module and plant power flow evaluation module. In the engineering design module, the maximum magnetic field on the helical coil B_{max} and the stored magnetic energy of the coil system W_{mag}, both are quite important parameters to evaluate the engineering design feasibility, and are estimated using the input data of the helical coil geometry. Since a calculation for B_{max} is time consuming, HELIOSCOPE evaluates B_{max} using the power law scaling with engineering parameters developed in another study [6]. W_{mag} is directly calculated using Neumann's law with a simplified model of coils. The blanket space is obtained as the minimum distance between the surface of the plasma facing side of the inboard helical coil and the field line in the ergodized layers on the equatorial plane at the vertically elongated cross-section. The poloidal cross-sectional shape of the helical coils is calculated considering the current density and width-to-height ratio of the helical coils. Consequently, a reasonably accurate evaluation with short calculation time sufficient for parametric scans can be realized. In the physics design module, plasma performance is evaluated by a simple 0D (volume-averaged) power balance model:

$$\mathrm{d}W_p/\mathrm{d}t = -W_p/\tau_E - P_{rad} + \eta_\alpha P_\alpha + P_{aux} = 0, \qquad (1)$$

where W_p, τ_E, P_{rad}, P_α , P_{aux} and η_α are the plasma stored energy, energy confinement time, radiation loss, alpha heating power, auxiliary heating power and alpha heating efficiency, respectively. In the calculation, the electron temperature and density profiles are described as a power of the parabolic function of the normalized minor radius ρ; $T_e = T_{e0}(1-\rho^2)^{\alpha_T}$ and $n_e = n_{e0}(1-\rho^2)^{\alpha_n}$. The temperature equality between electrons and ions ($T_e = T_i$) and the charge neutrality condition are assumed. The values of electron temperature and density on the axis, fractions of impurity ions to electrons and alpha heating efficiency η_α are given as input parameters. Then the required confinement time τ_E to achieve a steady-state power balance can be derived from equation (1) and the required confinement improvement is obtained using the ISS04v3 confinement scaling [7]. The Sudo density limit [8] is used as a physics constraint. In the plant power flow evaluation module, neutron and thermal loads on the first wall and divertor plates, plant thermal output, gross and net electric output are estimated. In the evaluation of the averaged neutron wall load on the first wall, a conservative evaluation using the total surface area of the plasma is performed.

3. Parametric scan

Using HELIOSCOPE, parametric scans were carried out with three cases of $\gamma = 1.15$, 1.20 and 1.25. In this study, the following three engineering constraints were considered: the inboard minimum blanket space $\Delta_{\rm in}$, averaged neutron wall loading $\langle\Gamma_{\rm nw}\rangle$ and stored magnetic energy $W_{\rm mag}$. According to neutronics calculations in the past design studies, a blanket with a thickness of $\sim$1 m is necessary to achieve a sufficient tritium breeding ratio (TBR) over 1.05 and the effective shielding of superconducting coils from fast (>0.1 MeV) neutrons with the standard design of Flibe (LiF + BeF_2) + Be/JLF-1 blanket [2]. In the design study of FFHR, a spectral shifter and tritium breeding (STB) blanket has been proposed [9]. This blanket concept enables a long-term operation without a replacement of the structural material if the averaged neutron wall loading $\langle\Gamma_{\rm nw}\rangle \leqslant 1.5\,{\rm MW\,m^{-2}}$. On the other hand, a detailed structural analysis is required to determine the maximum limit of $W_{\rm mag}$. In a past design study, $W_{\rm mag}$ = 120–140 GJ is considered to be achieved with a small extension of the ITER technology [10]. Here we give 160 GJ as an indicator of the capability of R&D optimization with the same level of technical base. Therefore, these three constraints, $\Delta_{\rm in} \geqslant 1.0$ m, $\langle\Gamma_{\rm nw}\rangle \leqslant 1.5\,{\rm MW\,m^{-2}}$ and $W_{\rm mag} \leqslant 160$ GJ, were adopted in this study. The current density of helical coils is fixed at 25 A mm^{-2} throughout this study.

In this study, an inward-shifted plasma configuration ($R_{\rm ax}/R_{\rm c}$ = 3.6/3.9) was adopted. In LHD, this inward-shifted configuration observes relatively good confinement [7]. Figures 5, 6 and 7 show the design window on the plane of $R_{\rm c}$ and $B_{\rm t,c}$ (toroidal field averaged over one helical pitch along the winding centre of the helical coils) for the case of $\gamma = 1.25$, 1.20 and 1.15, respectively. All design points in figures 5–7 satisfy the self-ignition condition and have a constant fusion power of $P_{\rm fus}$ = 3 GW, which is required to obtain an electric output comparable to current large-scale power plants ($\sim$1 GWe) with a thermal efficiency of $\sim$40%. We also assumed the following physics conditions: line-averaged electron density of 1.5 times the Sudo density limit, density and temperature profile factors of $\alpha_n = 0.25$ and $\alpha_T = 0.75$, helium and oxygen ion fraction of 3% and 0.5%, respectively. The shaded region in figures 5–7 corresponds to the design window that satisfies all the engineering constraints: $\Delta_{\rm in} \geqslant$ 1.0 m, $W_{\rm mag} \leqslant$ 160 GJ and $\langle\Gamma_{\rm nw}\rangle \leqslant 1.5\,{\rm MW\,m^{-2}}$. Contours of the volume-averaged beta value $\langle\beta\rangle$ and the required confinement improvement relative to LHD experiments $H^{\rm LHD}$ (corresponds to the confinement improvement factor relative to the ISS04v3 scaling with the renormalization factor of $f_{\rm ren}$ = 0.93) are also drawn in figures 5–7. It is clear that the boundary of the design window is determined mainly by the constraints of $\Delta_{\rm in}$ and $W_{\rm mag}$. Since these two parameters are the function of engineering parameters only, the possible design window on the $R_{\rm c}$–$B_{\rm t,c}$ plane is determined mainly by selecting γ. Note that larger values of both $H^{\rm LHD}$ and $\langle\beta\rangle$ are required for selecting the design points located on the lower side of the window. Therefore, the design points on

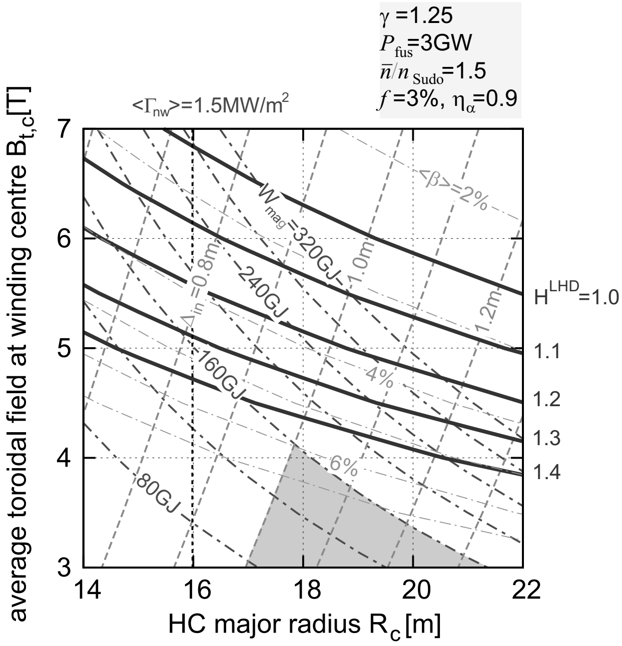

Figure 5. Contour map of design parameters for the case of $\gamma = 1.25$ and $P_{\rm fus}$ = 3 GW. The shaded region corresponds to the design window that satisfies all engineering and physics constraints.

the upper side of the window are favourable in terms of the core plasma design. Apparently, a reduction in γ expands the blanket space. The minimum inboard blanket space in the case of $\gamma = 1.15$ is $\sim$15 cm larger than that in the case of $\gamma = 1.25$ when the values of $R_{\rm c}$ and $B_{\rm t,c}$ are the same. The stored magnetic energy also reduces slightly with decreasing γ when the values of both $R_{\rm c}$ and $B_{\rm t,c}$ are maintained. On the other hand, the required confinement improvement becomes large with decreasing γ (corresponding to the upward shift of the contours of $H^{\rm LHD}$). This is because the averaged minor radius $\langle a_{\rm p}\rangle$ decreases with decreasing γ, while the energy confinement time is proportional to $\langle a_{\rm p}\rangle^{2.28}$. In the case of γ = 1.25, the design window is significantly limited by $\Delta_{\rm in}$. Since $W_{\rm mag}$ is proportional to $R_{\rm c}^3 B_{\rm t,c}^2$ and the energy confinement time τ_E is proportional to $R_{\rm c}^{0.64} B_{\rm t,c}^{0.84}$, the required $H^{\rm LHD}$ value increases with the increase in $R_{\rm c}$ if $W_{\rm mag}$ is fixed. Consequently, there is no design window with $H^{\rm LHD} < 1.4$ in the case of $\gamma = 1.25$. On the other hand, the design windows for the other two cases spread to the region with smaller values of $H^{\rm LHD}$. However, the design window is limited by $\langle\Gamma_{\rm nw}\rangle$ in the case of $\gamma = 1.15$. Therefore, the achievable minimum value of $H^{\rm LHD}$ and $\langle\beta\rangle$ in the case of $\gamma = 1.15$ is rather larger than those in the case of $\gamma = 1.20$. In this respect, $\gamma = 1.20$ is the optimum selection in the case of $P_{\rm fus}$ = 3 GW.

The relation between γ and $H^{\rm LHD}$ varies if a change in the value of $P_{\rm fus}$ is allowed. In the case of a higher fusion power, the contours of $H^{\rm LHD}$ shift downwards. However, the contours of $\langle\Gamma_{\rm nw}\rangle$ show a rightward shift and limit the design window significantly. Therefore, there is no design window with $H^{\rm LHD} < 1.4$ irrespective of the value of γ in the case of $P_{\rm fus} \geqslant$ 4 GW. On the other hand, the neutron wall load no longer limits the design window in the case of a lower fusion power. Figures 8, 9 and 10 show the design window

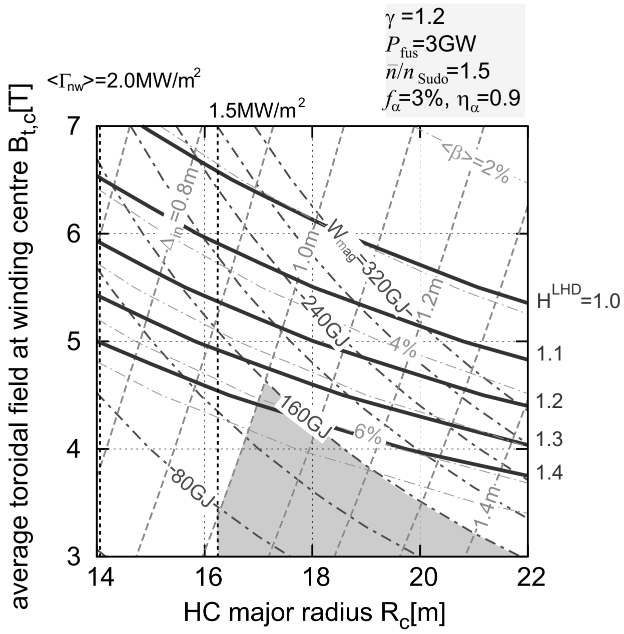

Figure 6. Contour map of design parameters for the case of $\gamma = 1.2$ and $P_{\rm fus} = 3$ GW. The shaded region corresponds to the design window which satisfies all engineering and physics constraints.

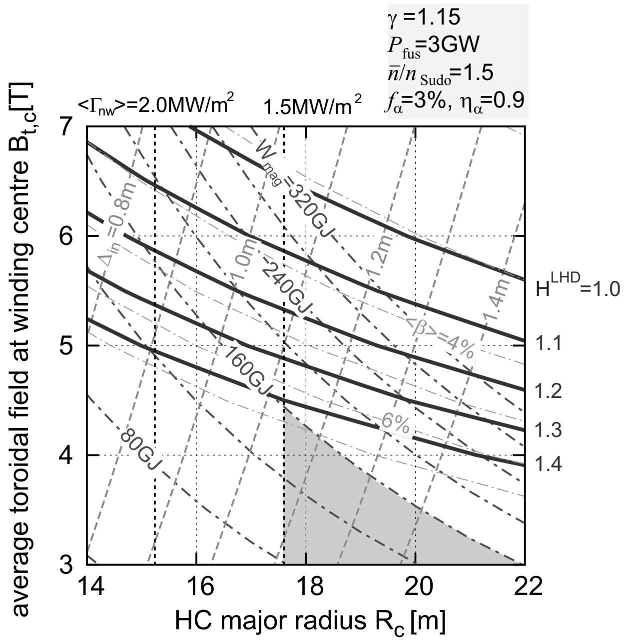

Figure 7. Contour map of design parameters for the case of $\gamma = 1.15$ and $P_{\rm fus} = 3$ GW. The shaded region corresponds to the design window which satisfies all engineering and physics constraints.

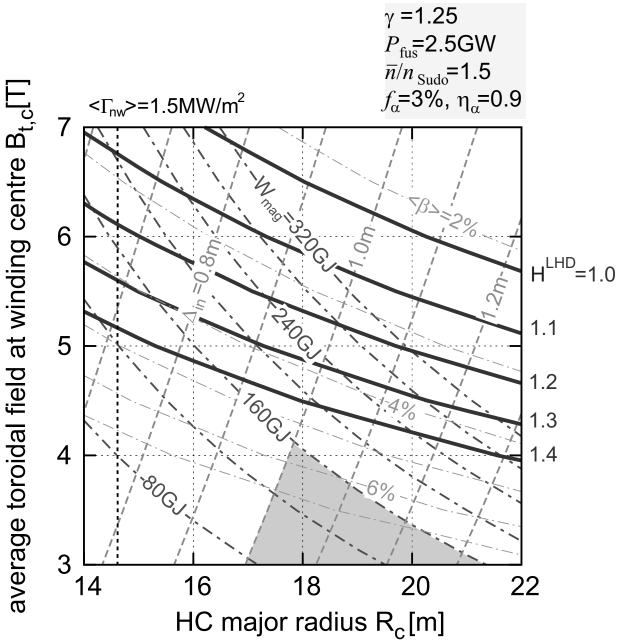

Figure 8. Contour map of design parameters for the case of $\gamma = 1.25$ and $P_{\rm fus} = 2.5$ GW. The shaded region corresponds to the design window which satisfies all engineering and physics constraints.

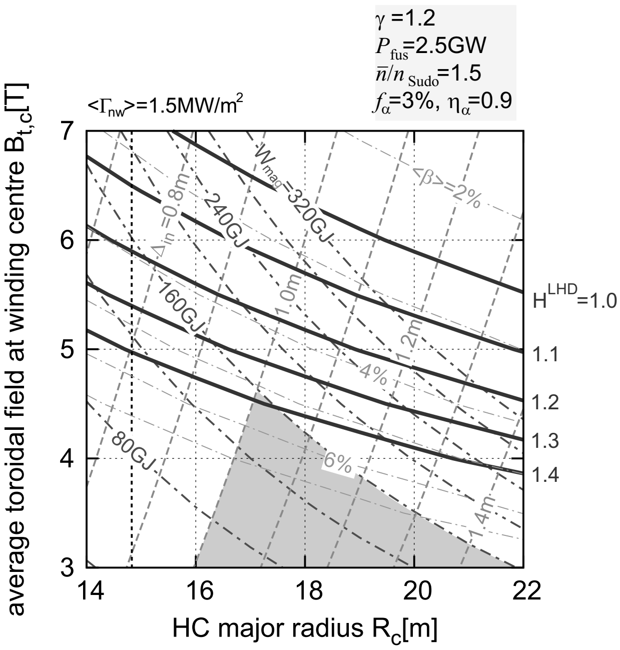

Figure 9. Contour map of design parameters for the case of $\gamma = 1.2$ and $P_{\rm fus} = 2.5$ GW. The shaded region corresponds to the design window which satisfies all engineering and physics constraints.

with $P_{\rm fus} = 2.5$ GW for the case of $\gamma = 1.25$, 1.20 and 1.15, respectively. In the case of $\gamma = 1.25$ and 1.20, the upper boundary of the design window on the $R_{\rm c}$–$B_{\rm t,c}$ plane is the same as that in the case of $P_{\rm fus} = 3$ GW because it is not restricted by $\langle\Gamma_{\rm nw}\rangle$. Therefore, the achievable minimum $H^{\rm LHD}$ value becomes larger. In contrast, the achievable minimum $H^{\rm LHD}$ with $P_{\rm fus} = 2.5$ GW is smaller than that with $P_{\rm fus} = 3$ GW in the case of $\gamma = 1.15$. This achievable minimum $H^{\rm LHD}$ in the case of $\gamma = 1.15$ with $P_{\rm fus} = 2.5$ GW is also smaller than that in the case of $\gamma = 1.20$ with the same $P_{\rm fus}$. This is because of the parameter dependence of the Sudo density limit. The Sudo density limit is proportional to $(B_{\rm ax}P_{\rm abs}/\langle a_{\rm p}\rangle^2/R_{\rm ax})^{0.5}$, where $B_{\rm ax}$ and $P_{\rm abs}$ are the magnetic field on the axis ($B_{\rm ax} = B_{\rm t,c}R_{\rm c}/R_{\rm ax}$) and the total absorbed power, respectively. Since $\langle a_{\rm p}\rangle$ in the case of $\gamma = 1.15$ is

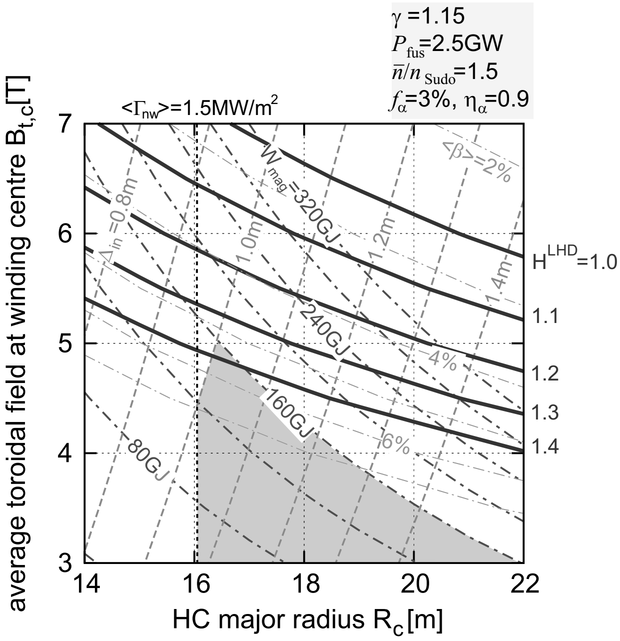

Figure 10. Contour map of design parameters for the case of $\gamma = 1.15$ and $P_{\text{fus}} = 2.5$ GW. The shaded region corresponds to the design window which satisfies all engineering and physics constraints.

smaller than that in the case of $\gamma = 1.20$ and P_{abs} correlates strongly with P_{fus}, the achievable density is larger in the case of $\gamma = 1.15$. The ISS scaling predicts that the confinement time is proportional to $n_e^{0.54} B^{0.83}$, while the achievable maximum $B_{t,c}$ with a constant value of W_{mag} becomes large with decreasing γ. The confinement enhancement effect by these two factors exceeds the degradation effect due to the decrease in the plasma volume. Consequently, $\gamma = 1.15$ can be a possible selection if $P_{\text{fus}} = 2.5$ GW is accepted.

Since design windows are quite sensitive to the engineering constraints, a small change in those constraints moderates the physics requirements significantly. In particular, a higher $\langle \Gamma_{\text{nw}} \rangle$ can be achieved by the use of advanced materials (tungsten carbide, vanadium alloy, etc). In this respect, further detailed studies on design feasibility of engineering components (first wall, blanket and superconducting coils) are required to optimize the value of γ. In this study, the same plasma properties (density and temperature profile, fraction of impurity ions, alpha heating efficiency) were assumed. If the temperature profile becomes more peaked or the density profile becomes less peaked, the restriction of the design window due to the density limit becomes more significant. In such cases, the design with a lower γ has an advantage in that it is less affected by the density limit. Although the ISS04v3 scaling was used for the evaluation of plasma confinement property, the effect of γ was not reflected in the renormalization factor for the LHD-type heliotron configuration. If these physics conditions depend on γ, the optimum value of γ can be varied from the above discussion. Consequently, the effect of γ on both energy and particle confinement also needs to be clarified to deepen the analysis.

4. Conclusion

A system design code for heliotron reactors, HELIOSCOPE, was developed and parametric scans were carried out in order to analyse the effect of helical pitch parameter γ on the design window of LHD-type heliotron reactors. It became clear that the design window of LHD-type heliotron reactors depends significantly on the engineering constraints: the minimum inboard blanket space, the stored magnetic energy and the averaged neutron wall load. In the case of the fusion output of 3 GW, $\gamma = 1.20$ is optimum for relaxing physics requirements. But the required confinement improvement in the case of $\gamma = 1.15$ is smaller than that in the case of $\gamma = 1.20$ if the design window is not restricted due to the neutron wall load. Therefore, $\gamma = 1.15$ is also a possible candidate if a fusion power of $\leqslant 2.5$ GW or a neutron wall load > 1.5 MW m^{-2} is accepted. The possible design window can be expanded by the progress in engineering research and development. Therefore, a further detailed study on design feasibility of engineering components (first wall, blanket and superconducting coils) is required to optimize the value of γ. The effect of γ on the physics conditions (density and temperature profiles, fractions of impurity ions, alpha heating efficiency, energy and particle confinement properties) also needs to be clarified to deepen the analysis.

Acknowledgments

The authors appreciate Drs O. Mitarai, S. Sudo, T. Watanabe, J. Miyazawa, T. Tanaka Y. Kozaki and O. Motojima, and other members of FFHR Design Group for giving valuable comments and advice.

References

[1] Komori A. *et al* 2010 *Fusion Sci. Technol.* **58** 1
[2] Sagara A. *et al* 2008 *Fusion Eng. Des.* **83** 1690
[3] Hirshman S.P. *et al* 1983 *Phys. Fluids* **26** 3553
[4] Suzuki Y. *et al* 2006 *Nucl. Fusion* **46** L19
[5] Watanabe K.Y. *et al* 2010 *Fusion Sci. Technol.* **58** 160
[6] Goto T. *et al* 2009 *Fusion Sci. Technol.* **56** 925
[7] Yamada H. *et al* 2005 *Nucl. Fusion* **45** 1684
[8] Sudo S. *et al* 1990 *Nucl. Fusion* **30** 11
[9] Sagara A. *et al* 2005 *Nucl. Fusion* **45** 258
[10] Imagawa S. *et al* 2009 *Nucl. Fusion* **49** 075017